Food Hydrocolloids 137 (2023) 108373

Contents lists available at ScienceDirect

Food Hydrocolloids

journal homepage: www.elsevier.com/locate/foodhyd

Association of caseins with β-lactoglobulin influenced by temperature and calcium ions: A multi-parameter analysis

Hossein Mohammad-Beigi [a,**], Wahyu Wijaya [a], Mikkel Madsen [a], Yuya Hayashi [b,c], Ruifen Li [d], Tijs Albert Maria Rovers [e], Tanja Christine Jæger [f], Alexander K. Buell [g], Anni Bygvrå Hougaard [d], Jacob J.K. Kirkensgaard [d,h], Peter Westh [i], Richard Ipsen [d], Birte Svensson [a,*]

[a] Enzyme and Protein Chemistry, Department of Biotechnology and Biomedicine, Technical University of Denmark, Søltofts Plads, Building 224, 2800, Kgs Lyngby, Denmark
[b] Department of Molecular Biology and Genetics, Aarhus University, Universitetsbyen 81, 8000, Aarhus C, Denmark
[c] Interdisciplinary Nanoscience Center (iNANO), Aarhus University, Gustav Wieds Vej 14, 8000, Aarhus C, Denmark
[d] Department of Food Science, University of Copenhagen, Rolighedsvej 26, 1958, Frederiksberg C, Denmark
[e] Arla Foods a.m.b.a, Agro Food Park 19, 8200, Aarhus, Denmark
[f] Arla Foods Ingredients Group P/S, Sønderupvej 26, 6920, Videbæk, Denmark
[g] Protein Biophysics, Department of Biotechnology and Biomedicine, Technical University of Denmark, Søltofts Plads, Building 227, 2800, Kgs. Lyngby, Denmark
[h] Niels Bohr Institute, Faculty of Science, University of Copenhagen, Blegdamsvej, 172100, Copenhagen, Denmark
[i] Interfacial Enzymology, Department of Biotechnology and Biomedicine, Technical University of Denmark, Søltofts Plads, Building 224, 2800, Kgs. Lyngby, Denmark

ARTICLE INFO

Keywords:
Aggregation propensity
β-lactoglobulin
Caseins
Chaperone
Milk
Colloidal stability

ABSTRACT

Aggregation of the major whey protein in bovine milk, β-lactoglobulin (β-Lg) is strongly influenced by association with caseins (CNs). Here, by using combined differential scanning fluorimetry and dynamic light scattering, the conformational stability and aggregation propensity of β-Lg and three types of CNs (α, β and κCNs) as well as their mixture have been systematically evaluated at different temperatures and Ca^{2+} concentrations in a multi-parametric approach. While β-Lg was affected significantly through denaturation and resulting aggregation by heat treatment with little dependency on Ca^{2+}, αCN and βCN were influenced considerably by Ca^{2+}. Through modifying the aggregation of β-Lg, CNs showed a different chaperone-like activity among the three types which were markedly dependent on the temperature and Ca^{2+} concentration. The presence of CNs resulted in smaller mixed aggregates compared to pure β-Lg aggregates, mainly through interaction of CNs with unfolded β-Lg and also by influencing the process of β-Lg unfolding. This was further confirmed by small angle X-ray scattering and isothermal titration calorimetry indicating that Ca^{2+} enhanced the interaction between β-Lg and CNs. Our experimental approach sheds light on molecular understanding of CN- β-Lg interactions and provides insight into how micro-structural assembly of milk proteins can be modulated to enable different functionalities in milk-based products.

1. Introduction

Interactions between caseins (CNs) and whey proteins during thermal processing of milk play a key role in the properties of dairy products. Milk and most beverages require heat treatment before sale or further processing (Etzel, 2004), which results in a number of physicochemical changes, including denaturation and aggregation of proteins (Durand, Gimel, & Nicolai, 2002). β-lactoglobulin (β-Lg) is the major whey protein (about 50%) in bovine milk and has a range of functionalities suitable for food and pharmaceutical applications, *e.g.* as an emulsifier (Li, Pan, Yang, Rao, & Chen, 2022) and wall material for encapsulation of bioactive compounds (Mekhloufi, Vilamosa, & Agnely, 2022; Zhang et al., 2022). During heat treatment, β-Lg undergoes conformational changes and aggregation, which are essential for some applications (*e.g.*, gelation), but in certain cases, the aggregation is undesirable since it can destabilize the resulting food products. CNs, in particular, are naturally non-structured proteins that form macromolecular assemblies (denoted micelles) in an aqueous solution. It was noticed in the early 1960s

* Corresponding author.
** Corresponding author.
E-mail addresses: hosmbe@dtu.dk (H. Mohammad-Beigi), bis@bio.dtu.dk (B. Svensson).

https://doi.org/10.1016/j.foodhyd.2022.108373
Received 19 August 2022; Received in revised form 25 November 2022; Accepted 29 November 2022
Available online 3 December 2022

Table 1
Parameters of fitting of SAXS data with a plugin model combining an ellipsoidal shape (protein structure) to 0.07 to 0.2 Å and a polydisperse spherical model to lower q range from 0.005 to 0.07 Å.

Protein Mixture	A_radius (nm)	A_scale * 104	B_scale * 104	B_radius_polar (nm)	B_radius_equatorial (nm)
αCN+β-Lg	29.6	1.5593	1.3777	3.89	3.89
βCN+β-Lg	16.4	3.1178	1.0191	1.95	4.21
κCN+β-Lg	19.6	5.5756	0.54	4.41	9.06

(Kenkare, Morr, & Gould, 1964) that CNs have chaperone-like behavior and can prevent aggregation of a number of proteins such as whey proteins, insulin, and ovalbumin and this versatility has been attributed to their highly flexible nature (Matsudomi, Kanda, Yoshika, & Moriwaki, 2004; Morgan, Treweek, Lindner, Price, & Carver, 2005; Yousefi et al., 2009).

Four types of CNs (α_{S1}-, α_{S2}-, β- and κCN) possess distinct primary structures and show different solubility in solutions containing calcium ions (Marchesseau et al., 2002). The inability of the CNs to form a stable tertiary structure stems from their high content of proline, which provides them with a flexible structure that renders them very susceptible to proteolysis (Fox, 2008). Additionally, post-translational modifications such as phosphorylation (in α_{S1}, α_{S2}, and βCN) and glycosylation (in κCN) lead to multiple proteoforms and heterogeneity for individual CNs (Fox, 2008). The combined features of CNs as lacking well-defined secondary structure and having exposed hydrophobic residues confer a high surface activity (Li et al., 2022). Another interesting feature of CNs is the uneven distribution of the hydrophobic and polar residues (Fox & McSweeney, 2013), giving them an amphiphilic structure. Accordingly, different biophysical techniques are required to analyze the micellar characteristics and association of the mixtures of different forms of caseins, i.e. monomer, oligomer, and fibrils (Portnaya, Khalfin, & Danino, 2021; Wijaya et al., 2020). The high surface activity and amphiphilic structure provide CNs with good foaming and emulsifying properties and make them functional proteins for food applications. The CNs are present as large protein complexes (micelles) in milk. α_S- and βCNs are assembled inside the micellar particles and stabilize the micelles through hydrophobic interactions as well as the interaction between their phosphoserine residues and calcium ions, while κCN is soluble in the presence of calcium ions and mostly situated on the micellar surface (Dalgleish & Corredig, 2012; Holt, Carver, Ecroyd, & Thorn, 2013). α_{S1}CN and βCN lack cysteine, whereas α_{S2}CN and κCN contain half-cystine residues engaged in intermolecular disulphide bonds and association with β-Lg (Fox, 2008).

β-Lg is a small globular protein with a molecular mass of 18.4 kDa, which is present in different oligomerization states depending on the solution conditions. At neutral pH, β-Lg exists in a monomer-dimer equilibrium (Mercadante et al., 2012), which shifts toward the monomer with increasing ionic strength and temperature (Uhrinová et al., 2000), and undergoes irreversible changes at temperatures between 70 and 140 °C (Iametti, De Gregori, Vecchio, & Bonomi, 1996). The aggregation of β-Lg is also influenced by environmental conditions such as temperature, ionic strength and the presence of other proteins (Erabit, Flick, & Alvarez, 2013; Haque & Kinsella, 1988; Rodrigues et al., 2020; Sava, Van der Plancken, Claeys, & Hendrickx, 2005). It is not elucidated if β-Lg aggregates during the unfolding of the molecule or only at the end of the unfolding process. During unfolding, β-Lg exposes free thiols and hydrophobic groups, which are believed to induce the formation of links between molecules through intermolecular disulphide bridges (Petit, Herbig, Moreau, & Delaplace, 2011).

In the last few decades, extensive research focused on understanding the association of milk proteins and their unfolding and aggregation during the heating processes by using a variety of techniques. Previous studies have shown that CNs can diminish the aggregation of β-Lg as seen by a decrease in turbidity during heating (Guyomarc'h, Nono, Nicolai, & Durand, 2009; Matsudomi et al., 2004; Morgan et al., 2005; Yousefi et al., 2009), but the mechanism is not fully understood. A chaperone can prevent aggregation and aid in refolding of proteins, but dependent on the type of proteins, CNs behave differently and in some cases cannot assist in protein refolding and only prevent aggregation of unfolded proteins. The chaperone moiety of CN micelles has been most frequently attributed to αCNs and βCNs (Morgan et al., 2005; Thorn et al., 2005; Yousefi et al., 2009). The hydrophilic domains of the CNs increase their solubility in aqueous media while their hydrophobic domains interact with partially unfolded β-Lg (Yousefi et al., 2009). Kehoe and Foegeding (2011) showed that βCN altered the heat-aggregation of β-Lg, as shown by a reduction in turbidity, through competing with whey proteins in the aggregation process, but differential scanning calorimetry (DSC) indicated that βCN did not alter the denaturation temperature of β-Lg (Kehoe & Foegeding, 2011). Furthermore, the same study showed that at 10 mM calcium chloride, chaperone activity of βCN was completely lost. Following this, Kehoe and Foegeding (2014) used transmission electron microscopy (TEM) to confirm that smaller and more regularly shaped aggregates formed when β-Lg was mixed with βCN, while the measured electrostatic properties of the final aggregates suggested that electrostatic stabilization was not the reason for the observed differences in aggregate size (Kehoe & Foegeding, 2014). Li et al. (Li, Pan, et al., 2022) used small angle X-ray scattering (SAXS) to show that the heat-induced denaturation and resulting aggregation of whey proteins is mainly a surface effect, leaving the overall protein shape unaffected, and that caseins remained largely unaffected. In addition, the interaction of β-Lg with CNs studied with graining incident SAXS (GISAXS) has shown that the core of the micelles becomes more compact as a result of preferential binding of β-Lg on the micellar surface (Steinhauer, Kulozik, & Gebhardt, 2014).

Although a wide range of different experimental techniques have been used to characterize the interaction of CNs and β-Lg, a single, recently developed microcapillary-based instrument platform, in which differential scanning fluorimetry is combined with dynamic light scattering (Prometheus Panta by Nanotemper), can address many of the central remaining questions on the protein mixtures' thermoresistance and colloidal stability, solution homogeneity, and aggregation propensity. Here, we introduced the use of this instrument through performing thermal ramps from 20 to 95 °C to gain knowledge about the conformational state, thermal stability, and aggregate formation of milk proteins and their various mixtures. Simultaneous measurement of these characteristics allows the possibility of considering any interference from the interaction of the particles on the scattering and fluorescence signals. The thermodynamic and structural properties of the protein mixtures were determined by isothermal titration calorimetry (ITC) and SAXS.

2. Materials and methods

2.1. Preparation of protein solutions

β-Lg isoform A was purified in-house from raw milk (Kristiansen, Otte, Ipsen, & Qvist, 1998) and found to be >95% pure as assessed by SDS-PAGE. αCN, βCN, and κCN from bovine milk (≥98, ≥70, and ≥70% protein, respectively) (Sigma Aldrich, St Louis, Missouri, USA) were used without further purification. Protein stock solutions (20 mg mL^{-1}) were prepared in 10 mM HEPES pH 7.0. β-Lg, αCN, βCN, and κCN concentrations were determined spectrophotometrically at 280 nm using molar extinction coefficients, ϵ, of 17,660, 25,900, 11,000 and 19,

035 $M^{-1}cm^{-1}$, respectively.

Mixtures of the CNs and β-Lg were prepared by diluting and mixing protein solutions in 10 mM HEPES pH 7.0 containing different concentrations of $CaCl_2$. For the experiments at 85 °C, molar ratios of β-Lg/αCN, β-Lg/βCN, β-Lg/κCN at 1:0.04, 1:0.2, 1:0.4, 1:0.8 were prepared at fixed β-Lg and $CaCl_2$ concentrations of 0.05 mM and 1 mM, respectively. Each mixture (2 mL) was transferred into a 4 mL glass vial for heat treatment (85 °C, 15 min) and subsequently immediately immersed in an ice-water bath for 10 min before performing further analysis.

2.2. Structure and scattering analysis of the proteins

The combined nano-differential scanning fluorimetry (nDSF), turbidity, and dynamic light scattering of the samples as a function of the protein and $CaCl_2$ concentration were carried out with a Prometheus Panta instrument (Nanotemper, Munich, Germany). The Prometheus Panta instrument provides simultaneous and multi-parametric assessments of structural integrity and colloidal stability of the proteins. Approximately 10 μL of each sample were loaded into microcapillaries and sealed with a specific sealing paste (Nanotemper, Munich, Germany) to prevent evaporation. The thermal unfolding profiles of proteins were measured by following the shift in the fluorescence emission spectra through the ratio of emission intensity at 330 and 350 nm (F350/F330) upon excitation at 280 nm caused by the change in the environment of the aromatic residues in the proteins. DLS was measured with a laser at 405 nm and turbidity with back reflection optics in the same capillaries. The experiments were performed by scanning from 20 to 95 °C and then cooling to 20 °C at a scan rate of 1.5 °C/min. The instrument software automatically determined the temperature of aggregation onset (T_{agg}) and cumulant radius. To determine the onsets of turbidity (aggregation onset) the software looks for the first two-state transition in the data. It then uses a linear fit on the baseline and a two-state fit on the transition. The onset corresponds to the temperature at which the two-state model fit deviates from the linear fit (baseline) by more than 0.5%. To calculate the onset of the cumulant radius increase (T_{size}) by the software, first, the initial radius or initial scattering intensity is calculated by a median fit to the initial data points (baseline). Second, the point of the curve is determined at which the radius or scattering intensity is increased by 10% (i.e. by a factor of 1.1). Third, the slope of the curve at this point is prolonged towards the baseline and the onset corresponds to the point, at which the slope intersects the baseline.

2.3. Isothermal titration calorimetry

Isothermal titration calorimetry (ITC) was performed using the NanoITC2G (TA Instruments, Delaware, USA). For binding of Ca^{2+} to milk proteins, the sample cell was filled with 0.05 mM β-Lg, αCN, βCN, κCN in 10 mM HEPES pH 7.0 (1000 μL), and the syringe with 50 mM $CaCl_2$ (250 μL). Binding between β-Lg and CNs at 85 °C was observed by titrating 0.05 mM CNs in 10 mM HEPES pH 7.0 in the absence and presence of 1 mM $CaCl_2$ with 30 injections of 6 μL of 1 mM β-Lg in the same buffer, each with a duration time of 2 s and a spacing time of 300 s. The solution in the cell was continuously stirred at 250 r.p.m. Heats of dilution were subtracted from the titration data using relevant control titrations.

2.4. Circular dichroism (CD) spectroscopy

CD spectroscopy was performed using a Jasco J-1500 spectropolarimeter (JASCO, Inc., Tokyo, Japan). The CD spectra of the β-Lg/βCN complexes were recorded between 190 and 250 nm at 25 °C, by scanning with a speed of 100 nm/min, 2 s response time, and 1 nm step size. β-Lg/βCN mixtures were diluted 10 times using deionized water. The samples were loaded into a rectangular quartz cuvette with a path length of 1 mm. The spectra of the three accumulated scans were averaged and corrected by subtracting the solvent/buffer spectra. The secondary structure of β-Lg/βCN complexes was predicted using the instrument software, Spectra Manager™ (Jasco Int, Tokyo, Japan).

2.5. Composition of heated-treated protein solutions

Protein complex aggregates generated by heating of β-Lg/CN mixtures were fractionated and characterized by size exclusion chromatography (SEC) using a Hi-load Superdex 200 prep grade (pg) 16/60 column equilibrated at a 1 mL/min flow rate with 10 mM HEPES pH 7.0 and an ÄKTA explorer system (GE Healthcare, Chicago, Illinois, USA). Approximately 0.5 mL sample was loaded onto the column and the molecular weights of the proteins in the eluted fractions were calculated based on the retention volumes of the proteins and the calibration curve.

2.6. Determination of protein profiles and composition of protein complex aggregates

SEC fractions (see 2.5) were applied on Mini-PROTEAN® TGX™ Precast Gels (4–20%, BIO-RAD, USA) under denaturing conditions to analyze the composition of each peak. β-Lg/CN complex samples were applied (30 μL) to the well of a precast gel and electrophoresis was run using Mini-PROTEAN® System at 200 V for 30 min. With at least two changes, gels were stained for 1 h using Coomassie Blue and destained by soaking for at least 2 h in 10% CH_3COOH, 50% CH_3OH, and 40% H_2O. To evaluate the approximate sizes of proteins, molecular weight markers (Mark 12™) for native and SDS-PAGE were run along with the samples.

2.7. Small-angle X-ray scattering (SAXS)

Mixtures of β-Lg/αCN, β-Lg/βCN, β-Lg/κCN were prepared by diluting and mixing protein solutions in 10 mM HEPES pH 7.0 containing 1 mM $CaCl_2$ to achieve mole-to-mole ratios of 1:1 for CNs and β-Lg at 0.1 mM β-Lg as fixed concentration. Each mixture (2 mL) was transferred into a 4 mL glass vial for heat treatment (85 °C, 15 min). Subsequently, the mixtures were immediately immersed in an ice-water bath for 10 min before SAXS analysis.

SAXS was measured using a Nano-inXider instrument from Xenocs SAS (Grenoble, France) having a 40 W micro-focused Cu source (Rigaku-Denki, Co., Tokyo, Japan) producing X-rays with a wavelength $\lambda = 0.154$ nm. The Nano-InXider has a Pilatus 100 k pixel-detector from Dectris (Baden, Switzerland) measuring the scattering in a q-range from 0.005 to 0.3 $Å^{-1}$, where the scattering vector $q = 4\pi\sin\theta/\lambda$ and 2θ is the scattering angle. 2D detector images were azimuthally averaged to produce 1D intensity curves as a function of q. Samples were measured in borosilicate capillary tubes with an inner diameter of 1.48 mm and the scattering from the buffer background was subtracted before analysis. Samples and backgrounds were measured for 45 min each. All background subtraction and initial data reduction were performed using the XSACT software package, including a logarithmic re-binning of the data.

All the SAXS data are presented in log I(q)- log q plots. Variation of scattering intensity I(q) within the sample can be calculated by:

$$I(q) = \Delta\rho^2 n_p V_p^2 P_p(q) S(q)$$

where $\Delta\rho^2$, n_p, V_p, and $P_p(q)$ are the contrast, number density, volume and form factor of the particle in question, respectively; q is the length of the scattering factor, and $S(q)$ is the structure factor describing any interactions between particles. $S(q)$ equals 1 in a dilute system, which we will assume here.

Subsequent data analysis and model fitting was done using the Sasview package (http://www.sasview.org/). Two fitting models were used, a model of ellipsoids was applied during the higher q ranges from 0.07 to 0.2 $Å^{-1}$ and a polydisperse spherical model to describe the larger

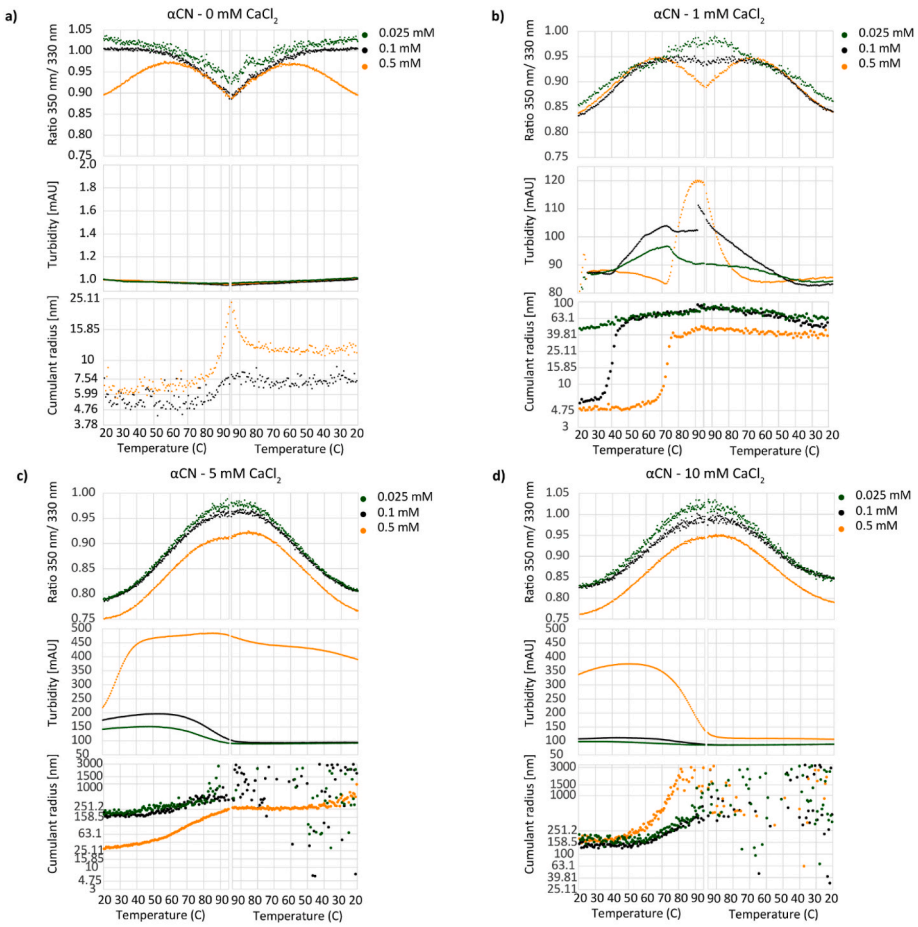

Fig. 1. Thermal stability and aggregation of αCN. Thermal unfolding followed by intrinsic fluorescence, turbidity, and dynamic light scattering of αCN (a) in the absence and in the presence of (b) 1 mM, (c) 5 mM, and (d) 10 mM $CaCl_2$ was measured by scanning in the range 20–95 and then 95-20 °C at 1.5 °C/min.

aggregates to fit the lower q range from 0.005 to 0.07 $Å^{-1}$

The equations for ellipsoid model are as follows (Feigin, Svergun, & others, 1987):

$$P(q,\alpha) = \frac{scale}{V} F^2(q,\alpha) + background$$

where.

$$F(q,\alpha) = \nabla\rho V \frac{3(\sin(qr) - qrcos(qr))}{(qr)^3}$$

and.

$$r = \left[R_e^2 \, sin^2\,\alpha + R_p^2 \, cos^2\,\alpha\right]^{\frac{1}{2}}$$

α is the angle between the axis of the ellipsoid and q, and $V=(4/3)\pi R_p R^2$ is the volume of the ellipsoid, Rp is the polar radius along the rotational axis of the ellipsoid, Re is the equatorial radius perpendicular to the rotational axis of the ellipsoid and $\Delta\rho$ (contrast) is the scattering length density difference between the scatterer and the solvent.

The following polydisperse sphere model was applied to the scattering data in the q range from 0.005 to 0.07 $Å^{-1}$ (Yang, Tyler, Ahrné, & Kirkensgaard, 2021).

$$P_{PS}(q) = \int P_S(q) D(R) V(R)^2 dR$$

where the monodisperse sphere form factor is given by.

$$P_S(q) = \left[3\frac{(\sin(qR) - qRcos(qR))}{(qR)^3}\right]^2$$

2.8. Principle component analysis

Principal component analysis (PCA) was performed on each protein dataset (αCN, βCN, κCN and β-Lg) to reduce dimensionality of the results and explore the relationship between protein/calcium concentrations and the responses quantified using Prometheus Panta (T_{agg}, I-Rad, I-Tur, E-Tur and P-Uns), Each dataset was log-transformed and scaled prior to PCA performed using the FactoMineR (ver. 2.4) (Lê, Josse, & Husson, 2008) package in the R environment (ver. 4.2.0). Resulting biplots were visualized using the factoextra (ver. 1.0.7) package color-coded separately for the two treatment groups (protein concentration and calcium concentration). In each plot, results obtained at the same concentration of protein or calcium were clustered by a convex hull to show the concentration-dependent patterns. The alpha value (transparency) of the arrows (variables) refers to the percentage contribution of the variable.

3. Results and discussion

3.1. The effect of protein and calcium concentrations on CNs and β-Lg properties

One of the most defining features of the CNs and whey proteins, which affect the final properties of the protein mixtures, is their

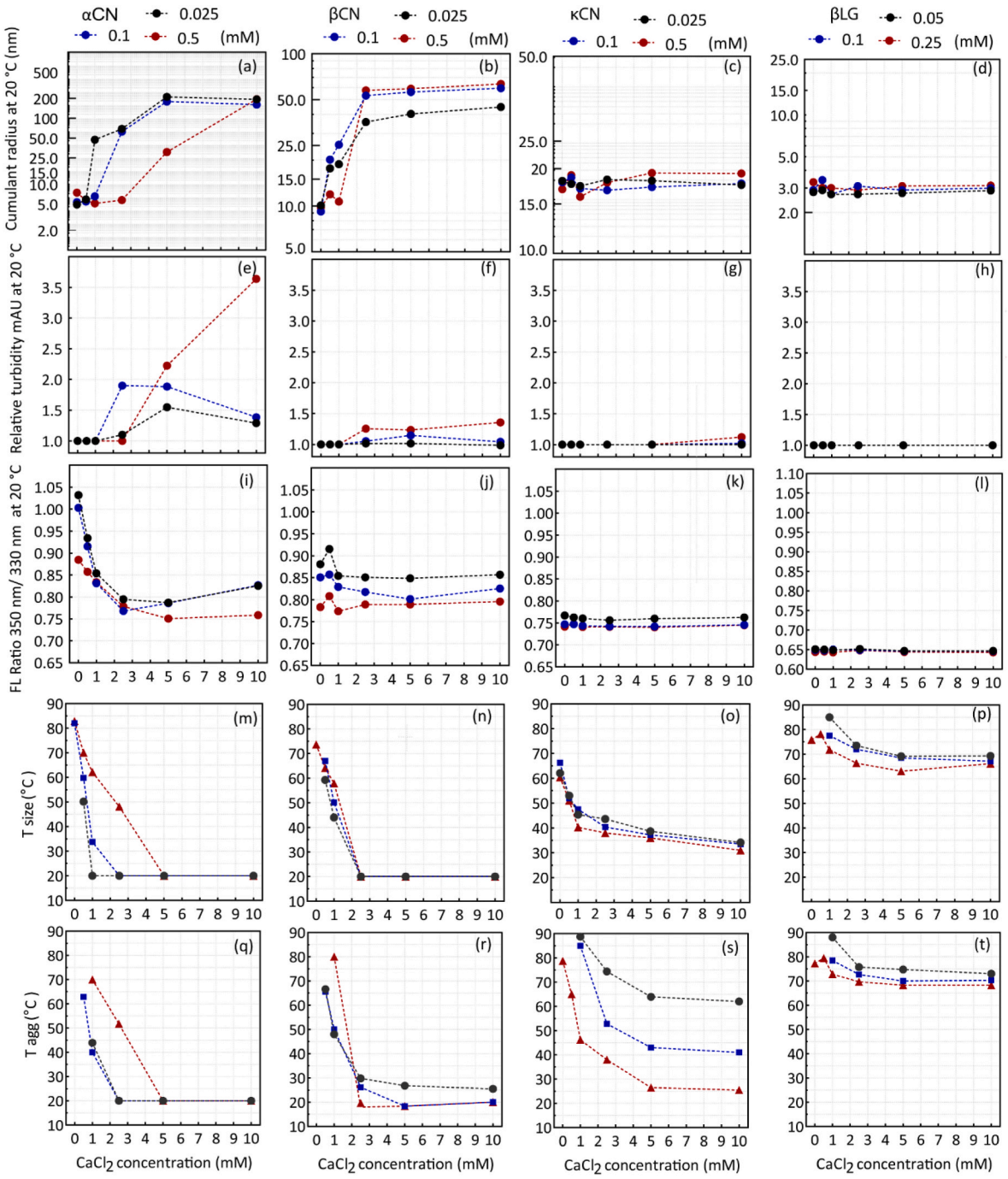

Fig. 2. Unfolding and size analysis of the proteins in the presence of $CaCl_2$ (0–10 mM). Cumulant radius of αCN (a), βCN (b), κCN (c) β-Lg (d). Relative turbidity of αCN (e), βCN (f), κCN (g) and β-Lg (h). Fluorescence ratio 350/330 nm of αCN (i), βCN (j), κCN (k) and β-Lg (l). The onset of increase in the cumulant size (Tsize) of αCN (m), βCN (n), κCN (o) and β-Lg (p) and Tagg of αCN (q), βCN (r), κCN (s) and β-Lg (t). The size of the aggregates in the presence of Ca^{2+} was compared to that in the absence of Ca^{2+}. Accordingly, Tsize = 20 °C and Tagg = 20 °C for the conditions in the presence of Ca^{2+} in Fig. 2 m-t indicate that the proteins are already aggregated before the heating process. However, they show a distinct onset of further aggregation at higher temperatures. These parameters were measured by heating the proteins from 20 to 95 °C in the presence of $CaCl_2$ (0–10 mM). The concentration of CNs and β-Lg was 0.025–0.5 mM and 0.05–0.25 mM, respectively. The change in the protein structure and size of the proteins by heating and cooling processes are shown in Figs. S1–S3.

temperature-induced aggregation behavior in solution (Anema, 2021; Li et al., 2019). Some protein solutions become turbid upon heating above 90 °C. To determine the thermal stability, the proteins in HEPES buffer at pH 7 and at different concentrations (CNs 0.025–0.5 mM; β-Lg 0.05–0.25 mM) in the presence of $CaCl_2$ (0–10 mM) were heated from 20 to 95 °C at a scan rate of 1.5 °C/min. To evaluate the degree of refolding and reversibility of the assembly and/or aggregation of the micelles and β-Lg, the samples were subsequently cooled to 20 °C at the same scan rate (1.5 °C/min). An example of such experiments (for αCN) is shown in Fig. 1 and for the rest of the proteins in Figs. S1–S3. We extracted different information from this data, i.e. initial cumulant radius (I-Rad) and turbidity (I-Tur), turbidity at 95 °C (E-Tur), the temperature at which the average particle size began to increase, T_{size}, the onset temperature of heavy aggregation, T_{agg}, and ratio of emitted fluorescence intensities at 350 and 330 nm at 20 °C, which allows determining the thermal stability of the proteins (P-Uns) (Fig. 2 and Fig. S4). T_{size}

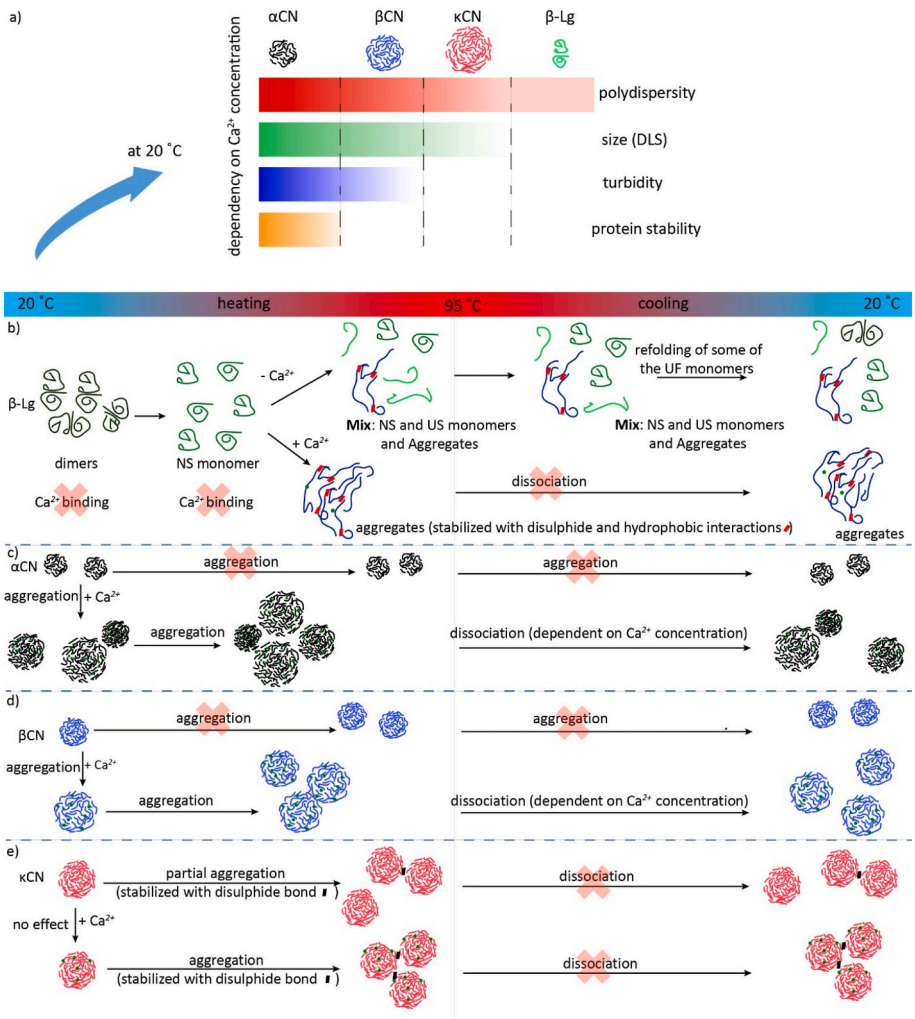

Fig. 3. Schematic representation of the effect of Ca^{2+} on heat denaturation and aggregation of β-Lg and the CNs. Comparison of the dependency of unfolding and size of the proteins on Ca^{2+} at 20 °C (a). The dark and light colors in the color gradient indicate the highest and lowest Ca^{2+} effect on the property, respectively. Properties of αCN and β-Lg show the highest and lowest dependency on Ca^{2+} at 20 °C. Heat denaturation and aggregation of β-Lg (b), αCN (c), βCN (d), κCN (e) in the presence of Ca^{2+}. Ca^{2+} only binds the unfolded β-Lg, induces aggregation and shifts the equilibrium toward unfolded protein. Heating leads to the formation of highly stable β-Lg and κCN aggregates via disulphide covalent bond formation, which do not dissociate after cooling down. Ca^{2+} leads to the formation of polydisperse αCN and βCN micelles, but it has slight effect on the stability of the micelles and after cooling, the turbidity decreases. NS: Native state; US: Unfolded state. (For interpretation of the references to color in this figure legend, the reader is referred to the Web version of this article.)

obtained by DLS exhibits the tendency of micelles to aggregate, which can correlate with thermal unfolding of proteins. The measured parameters varied greatly between the samples, suggesting that they represent a useful set of quantities to discriminate the different behavior between the investigated conditions.

In aqueous solutions, the CNs exist as monomer, micelle, or aggregated micelles dependent on the protein concentration, temperature, and Ca^{2+} concentration (Dauphas et al., 2005). To compare the overall patterns of protein properties between different protein and Ca^{2+} concentrations, a principle component analysis (PCA) was performed for the measured responses to changes in temperature (supplementary note and Figs. S5 and S6). The effect of Ca^{2+} and protein concentrations were clearly explained by the first two principal components (PC1 and PC2) in all protein types tested. In general for the CNs, PC1 and PC2 explained differences related to Ca^{2+} and proteins concentrations, respectively, underscoring the larger influence of Ca^{2+} concentrations than that of protein concentrations. Unlike the CNs, the first two PCs for β-Lg appeared opposite to those for the CNs, as anticipated from its little dependency on Ca^{2+}.

Detailed analysis of the data showed that at 20 °C and in the absence of Ca^{2+}, the micelle or protein size was the same, regardless of the protein concentration (Fig. 2a–d). Although κCN micelles have slightly larger initial radius at 20 °C (17–19 nm) than βCN (9–12 nm) and αCN (5–7 nm) in the absence of Ca^{2+}, their size remains between 16 and 20 nm even at 10 mM Ca^{2+}. The initial size of βCN and αCN is strongly influenced by the protein/Ca^{2+} ratio, which is dependent on the stoichiometry and correlated with the presence of respectively 5 and 10 phosphoserine (PS) groups on βCN and αCN. The ratio of $CaCl_2$ to PS is listed in Table S1. Ca^{2+} at low concentration, but at a molar ratio of at least 4 to αCN and βCN could increase the size of the micelles at lower protein concentration (0.025 mM). However, with increasing CNs concentration more Ca^{2+} albeit, at a lower ratio to PS (around 1), was required to increase the size of protein aggregates. As αCN contains more PS than βCN, higher Ca^{2+} concentration is required before the size of αCN is not changing anymore.

This pattern of Ca^{2+}-dependence is represented in the PCA analysis, where the positive correlation between Ca^{2+} and I-Rad appears stronger at higher Ca^{2+} concentrations (2.5–10 mM) particularly in the case of βCN (Fig. S5). On the other hand, lower Ca^{2+} concentrations (0–2.5 mM) were associated with negative PC1 scores based on high Tagg and/or P-Uns, indicating that αCN and βCN are intrinsically tolerant to high temperatures in the absence of Ca^{2+} while κCN did not show such a clear trend. The increase in the size of αCN and βCN by adding Ca^{2+} can stem from the combined effect of the Ca^{2+} bridging PS groups of proteins and shielding negative charges, together decreasing electrostatic repulsion (McSweeney & Fox, 2013). It should be noted that the polydispersity index (PDI) is protein dependent, and ranked in the following order αCN > βCN > κCN > β-Lg. The micelles are more polydisperse at higher protein concentrations (Fig. S7). In line with this observation, in PCA, E-Tur was in most cases positively correlated with an increase in the protein concentration at all Ca^{2+} concentrations (see Fig. S6, with a particular focus on the PC2).

Turbidity measurements provide an indication of the presence of large (100s of nm to micron-sized). The sample turbidity was quantified

by measuring the intensity of back-reflected, i.e. not scattered light, which depends on the concentration and size of aggregates. The sample turbidity increases upon heavy aggregation and/or significant increase in the size of the particles. The turbidity data at 20 °C (I-Tur) show the dependency of the aggregation of CNs and β-Lg on Ca^{2+} in the following order: αCN > βCN > κCN > β-Lg (Fig. 2 e-h). A comparison of the turbidity and DLS data can provide an overview on the population of small and big particles. While DLS can be biased by the presence of a small number of big particles, and provide the false impression of heavy aggregation, sample turbidity only increases noticeably when a significant fraction of the total protein has aggregated into large particles.

β-Lg and αCN contain 2 tryptophans, while βCN and κCN both only have one. The fluorescence ratio (F350/F330) at 20 °C (Fig. 2 i-l) was found to depend on the protein concentration and Ca^{2+} concentration in the following order: αCN > βCN > κCN > β-Lg (Fig. 2 i-l). The different fluorescence ratios observed at different protein concentrations under otherwise identical Ca^{2+} concentrations can be attributed to different relative populations of monomer and micelles. In contrast, β-Lg remains in the dimeric state even at higher concentrations, and thus the initial fluorescence ratio at 20 °C was found to be concentration-independent.

The fluorescence ratio can often be used to determine the fraction of unfolded protein at any point during the unfolding process. Environmental conditions such as temperature and the presence of Ca^{2+} can affect the protein aggregation, which will change the fluorescence of the proteins. Thus when evaluating the structural aspects of protein aggregation at different temperatures and Ca^{2+} concentrations, two factors are important, i.e. the change in the temperature and concentration and the spatial proximity of the proteins in micelles and/or aggregates, which is equivalent to an increase in their concentration (Faizullin, Konnova, Haertlé, & Zuev, 2013). Turbidity also can interfere with fluorescence measurement by causing light reflection and/or absorption. The dependency of unfolding and size of the proteins on Ca^{2+} at 20 °C shows the importance of recording the solution homogeneity and aggregation propensity simultaneously with fluorescence to improve the accuracy of the measurement. As summarized in Fig. 3a, by using combined differential scanning fluorimetry and dynamic light scattering, we showed that all properties of αCN measured at 20 °C before heating, were influenced considerably by Ca^{2+}, while only the size and polydispersity of κCN and only polydispersity of β-Lg were affected significantly by Ca^{2+} (indicated by dark colors in Fig. 3a). The number of Ca^{2+} binding amino acids (phosphoserines), plays an essential role in this observation at 20 °C, where the extent of the effect of Ca^{2+} on βCN and αCN is highly dependent on the protein/Ca^{2+} ratio and consequently on the stoichiometry.

3.2. Aggregation tendencies of CNs and β-Lg at high temperatures

In the next step, the aggregation tendency and unfolding of the proteins during heating to 95 °C followed by cooling to 20 °C was evaluated by measuring fluorescence ratio at 350 and 330 nm, turbidity, hydrodynamic radius (Fig. 1 and Figs. S1–S3), T_{size} (Fig. 2 m-p), and T_{agg} (Fig. 2 q-t). T_{size} obtained by DLS exhibits the tendency of proteins to aggregate and/or assemble, which can correlate with thermal unfolding of proteins.

The data show a strong dependency of T_{size} and T_{agg} for αCN on both Ca^{2+} and protein concentration, while those of βCN were highly dependent on the Ca^{2+} concentration and only weakly on the protein concentrations as indicated by PCA (Figs. S5 and S6). T_{size} and T_{agg} of κCN and β-Lg were slightly dependent on the $Ca^{2+}$and protein concentrations. We found a larger variation in the T_{agg} (Fig. 2 q-t) of the CNs compared to the dependency of T_{size} on the CNs and Ca^{2+} concentrations. The T_{agg} of αCN, βCN, and β-Lg is the same or slightly higher than their T_{size}, which shows that the formation of the first aggregates immediately leads to the formation of very large particles. In terms of κCN, at most protein and Ca^{2+} concentrations, T_{agg} was higher than T_{size}, which indicates that κCN micelles assembled successively into ever larger particles. Although the initial size of κCN and β-Lg at 20 °C was less affected by Ca^{2+} than that of βCN and αCN, both protein and Ca^{2+} concentrations influenced the final aggregate size of all CNs and β-Lg at 95 °C (Fig. 1 and Figs. S1–S3), but to different extent depending on the protein. The final size of αCN, βCN and β-Lg depended on both protein and Ca^{2+} concentrations, while the κCN concentration had only slight effect on the final size.

The effect of Ca^{2+} on the assembly of the CNs increased with increasing temperature, which is in agreement with earlier findings (Dauphas et al., 2005; Li et al., 2019). βCN and αCN were more affected by Ca^{2+} at both low and high temperatures, due to the PS groups, but at higher temperatures Ca^{2+} also affected κCN, probably due to the interaction with carboxylate groups and shielding of negative charges. Temperature seems to be more effective than Ca^{2+} in shifting the equilibrium toward micelles and aggregates by increasing the hydrophobicity and monomer density in the micelles (Fox & McSweeney, 2013).

The unfolding transition of proteins causes significant changes in the compactness of the proteins or induces protein aggregation (Duy & Fitter, 2006), which can affect the red shift in the tryptophan fluorescence emission spectrum observed during unfolding. Duy and Fitter showed that the red shift caused by the unfolding of α-amylases was influenced by the aggregation of the protein (Duy & Fitter, 2006). For β-Lg, under conditions where turbidity did not measurably increase, i.e. 0.05 and 0.1 mM β-Lg in the absence of Ca^{2+}, the fluorescence ratio increased without reaching a plateau until 95 °C and then decreased during subsequent cooling (Fig. S1). However, it did not reach the initial value, meaning that part of the protein molecules remained unfolded or associated in small aggregates. At higher β-Lg concentrations in the absence of Ca^{2+} and all protein concentrations in the presence of Ca^{2+}, both turbidity (E-Tur) and fluorescence ratio reached a plateau almost at the same temperature, indicating that all of the proteins were unfolded and aggregated irreversibly as both the fluorescence ratio and turbidity were unchanged even after cooling to 20 °C (summarized in Fig. 3b). Indeed, in PCA, what characterizes the PC1 of β-Lg responses is E-Tur showing a positive correlation to the increase in its protein concentration (Fig. S6), rather than to the change in the Ca^{2+} concentration (Fig. S5). Following the Le Chatelier's principle (Atkins & De Paula, 2013), the aggregation of the unfolded proteins will cause the folding equilibrium to shift towards the unfolded state. The high and slight dependency of respectively E-Tur and of T_{size} of β-Lg on Ca^{2+} confirms that Ca^{2+} has no effect on the unfolding of β-Lg and only induces the aggregation of unfolded β-Lg. Our finding is in accordance with results by Peixoto et al., where they showed that Ca^{2+} ions only bind to unfolded β-Lg at specific sites which might be a necessary feature to form the aggregates (Peixoto, Trivelli, André, Moreau, & Delaplace, 2018).

The CNs behave differently from β-Lg during the heating and cooling steps. The profile of turbidity and the fluorescence ratio of αCN and βCN appeared more symmetrical over the heating and cooling steps, showing formation of reversible protein assemblies at a high temperature which dissociate upon cooling (summarized in Fig. 3c–e). However, the temperature profile of the radius was not reversible which could be due to bias in DLS caused by the presence of low numbers of stable large particles. The change in the fluorescence ratio of αCN during the heating process is more pronounced than for βCN dependent on both protein and Ca^{2+}. The temperature profile of the fluorescence ratio during heating to 95 °C at different κCN and βCN concentrations was very similar, starting with a slight increase and then decreasing during heating to 95 °C; however, the cooling profile of κCN is not similar to its heating profile and the turbidity remains virtually constant at a high level even after cooling, which confirms irreversible formation of large aggregates at high temperatures, possibly due to disulphide bond formation (summarized in Fig. 3e).

Very little change in the secondary structure of βCN and κCN, as assessed by CD spectroscopy, suggests that the self-association of βCN and κCN even at high ionic strength and temperatures, did not cause

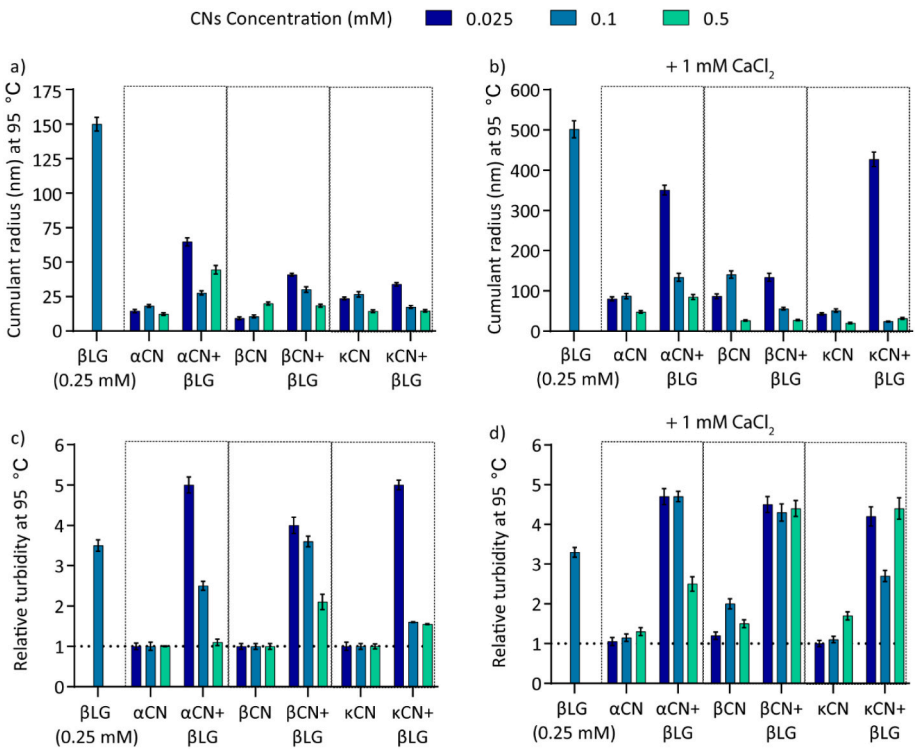

Fig. 4. Unfolding and size analysis of the CNs mixed with β-Lg in the presence of $CaCl_2$ (1 mM). Cumulant radius at 95 °C (a,b) and relative turbidity at 95 °C (c,d) in the absence and presence of 1 mM $CaCl_2$. The concentration of CNs and β-Lg was 0.025–0.5 mM and 0.25 mM, respectively.

significant change in their structural conformation, which is also consistent with previous results (Farrell, Qi, Wickham, & Unruh, 2002; Li et al., 2019). However, whilst the molecular structure appeared to be unchanged, their mean aggregate size was influenced by both Ca^{2+} and temperature, and increased probably due to Ca^{2+} bridges between otherwise unchanged micelles.

3.3. The association of CNs and β-Lg

It is known from previous studies that CNs can have a chaperone-like behavior and reduce aggregation of proteins (Matsudomi et al., 2004; Yousefi et al., 2009). We first studied the interactions between the CNs and β-Lg at different temperatures. Then, in order to better understand the interaction of β-Lg and CNs in the presence of Ca^{2+} as it will occur during milk pasteurization for yogurt manufacture, the protein mixtures were heated at 85 °C for 15 min and analyzed with different experimental methods. Visual observation of the protein mixtures are shown in Fig. S11.

3.3.1. Combined differential scanning fluorimetry and dynamic light scattering

At 95 °C, in the absence of Ca^{2+}, the size of the complex and turbidity depend on the CN concentration (Fig. 4a and b). By increasing CNs from 0.025 to 0.5 mM, the size and turbidity decreased, thus the CNs suppressed the aggregation of β-Lg.

Turbidity data (Fig. 4d) show that in the presence of 1 mM Ca^{2+}, CNs did not significantly prevent aggregation, but according to the DLS data (Fig. 4b), CNs- β-Lg associations led to the formation of smaller aggregates in the size range of pure CNs.

The fluorescence ratio and turbidity data showed that none of the assemblies formed between CNs and β-Lg was reversible after cooling to 20 °C, similarly to the irreversible aggregation observed of β-Lg and κCN alone (Figs. S8–S10).

3.3.2. Circular dichroism (CD)

CD data of 15 min heated β-Lg mixed with CNs at 85 °C in the presence of 1 mM Ca^{2+} at different molar ratios were collected (Fig. S12). β-Lg contains α-helix and β-sheet structures (Liyanaarachchi & Vasiljevic, 2018), while CNs lack defined secondary structures due to high proline content in their primary structure (Fox, 2008). The more random and unordered structures of the heated proteins at lower CNs/β-Lg ratios (Fig. S12e) may stem from formation of unstructured and unfolded proteins, while α-strand structures may arise by intermolecular hydrogen bonded anti-parallel β-sheet structures during protein aggregation (Clark, Saunderson, & Suggett, 1981). Higher CNs/β-Lg ratios still resulted in heat aggregation and denaturation of β-Lg but to a lesser extent as indicated by higher preserved helical structure and less random structures (Fig. S12f). The CNs can act in a number of different ways to bring about the reduction in size. According to the fluorescence ratio and CD data and previous reports (Kehoe & Foegeding, 2011), CNs slightly affect denaturation of β-Lg in the heating process, but the decrease in turbidity and size of the complex in the absence of Ca^{2+} and only the size of the aggregates in the presence of Ca^{2+} would be obtained mainly through the interaction between the micelles and denatured β-Lg.

It seems that the electrostatic interactions in addition to the amphiphilic nature of αCN and βCN are responsible for their chaperone-like activity (De & Rotello, 2008; Kehoe & Foegeding, 2011). However, for the interactions with κCN, the initial stages could be due to the electrostatic and hydrophobic interaction, which reduces the molecular proximity at the level (1–2 Å) required for disulphide bond formation (Haque & Kinsella, 1988) involved in the κCN - β-Lg complexation (McKenzie, Norton, & Sawyer, 1971), suggesting that κCN interacted with intermediate species of denatured β-Lg.

3.3.3. Size exclusion chromatography (SEC)

We compared the retention volume of CNs in SEC with globular protein standards (Fig. S13). The molecular weight of analyzed peaks for all samples is higher than of the protein monomers, demonstrating that

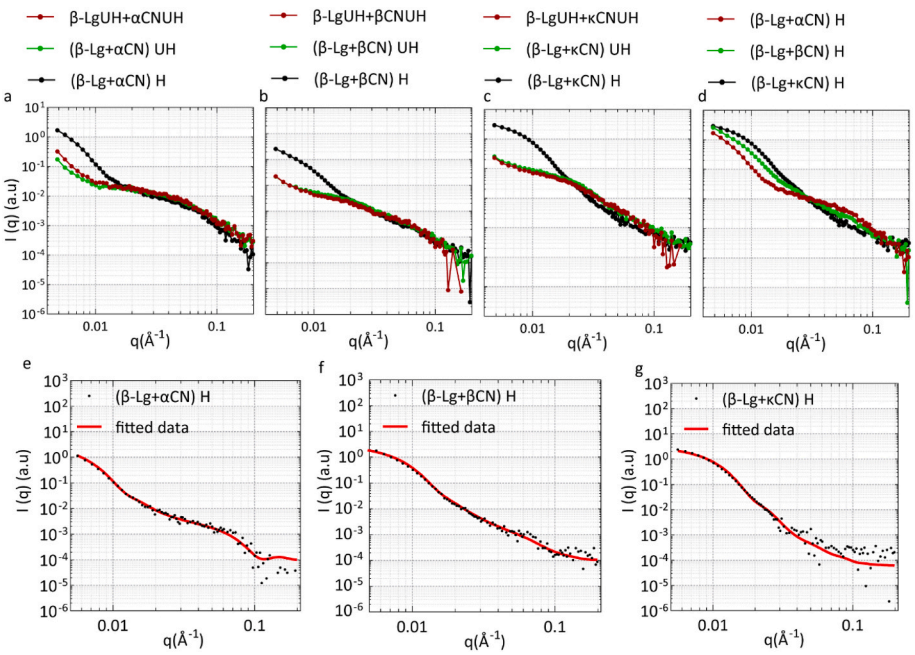

Fig. 5. Background-subtracted SAXS scattering pattern of protein mixtures. SAXS analysis of β-Lg mixed with αCN (a), βCN (b), and κCN (c) before and after heating at 85 °C for 15 min. Red line: sum of scattering of individual proteins before mixing and without heating, green line: mixtures before heating, black line: mixtures after heating. (d) Comparison of the scattering of the mixtures after heating. Fitting of SAXS data of mixtures of β-Lg with αCN (e), βCN (f), and κCN (g) after heating at 85 °C for 15 min with a plugin model combining an ellipsoidal shape (protein structure) and polydisperse spherical model. The parameters are listed in Table 1. (For interpretation of the references to color in this figure legend, the reader is referred to the Web version of this article.)

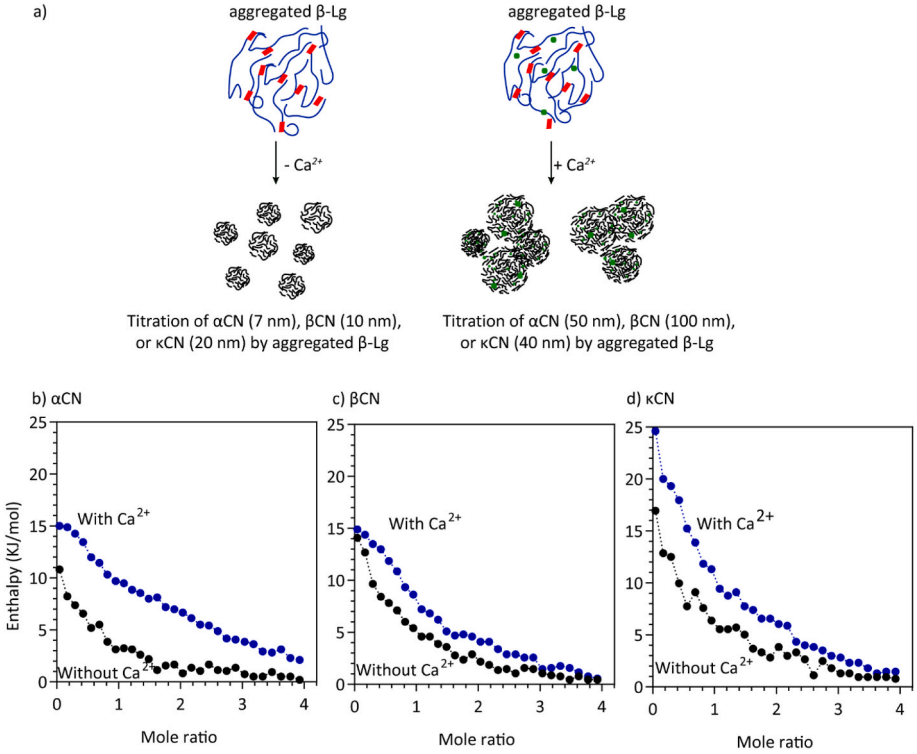

Fig. 6. Schematic representation of the titration of CNs by aggregated β-Lg in the presence and absence of Ca^{2+} (a). Integrated peak of ITC enthalpogram of 1 mg mL^{-1} of αCN (b), βCN (c), κCN (d) in 10 mM HEPES pH 7.0 in the absence and presence of 1 mM $CaCl_2$ titrated by 20 mg mL^{-1} β-Lg at 85 °C.

they were multimeric and no detectable monomer population was found in the solution. Two complexes were observed in the β-Lg samples mixed with αCN or βCN and both were larger than the protein monomers, while only one population was detected for the β-Lg mixed with κCN. The protein bands for β-Lg and the CNs are also shown in the inset of Fig. S13.

3.3.4. Small angle X-ray scattering (SAXS)

Fig. 5 represents an overview of the background-subtracted SAXS data of heated (H) β-Lg mixed with CNs. The overlapped summed scattering data of unmixed and unheated (UH) CNs and β-Lg (β-LgUH + CNsUH, red curve) and those of UH but mixed CNs and β-Lg ((CNs and β-Lg) UH, green curve) for the three CNs may confirm that there are no aggregates formed between the CN and β-Lg at room temperature, as they exhibited almost similar scattering curves in the low-q and intermediate-q range (0.004–0.02 $Å^{-1}$). DLS data also confirmed that no detectable aggregates were formed after mixing the CNs with β-Lg at room temperature.

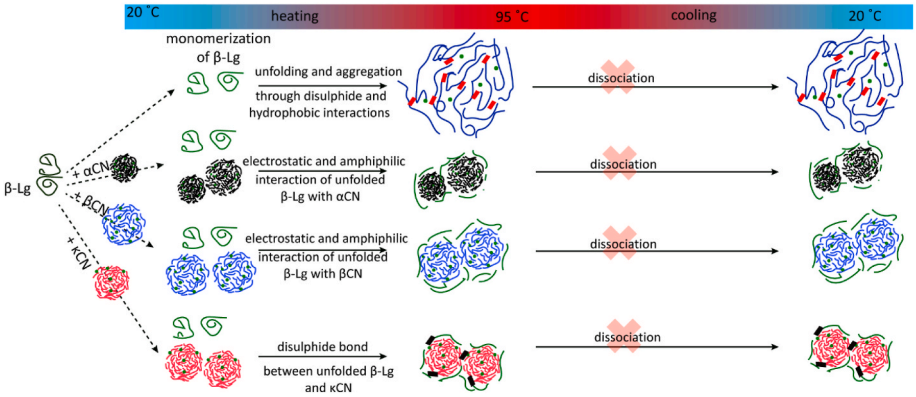

Fig. 7. Chaperone-like effects of CNs to reduce the aggregation of β-Lg. CNs reduce the aggregation of β-Lg through interaction with unfolded β-Lg. The aggregates formed between β-Lg and the CNs at high temperature are stable and do not dissociate upon cooling.

UH mixtures were compared with H mixtures to evaluate the effect of heating on their interaction. A combined model was fitted to the scattering data to describe the individual protein contour (model B) and the larger aggregates (model A) (Fig. 5 e-g). We see a significant change in the scattering data of the samples with heat treatment at low and high q. We used the ellipsoid model from SasView to represent the local shape of β-Lg, which changes in the unfolding process, in agreement with the data obtained on β-Lg oligomerization by high pressure (Minic et al., 2020). The B_scale which represents the local structure of β-Lg changes in the following order: αCN+ β-Lg> βCN+ βLG> κCN+ βLG, together with the scattering data confirms that the β-Lg structure is more preserved during heating when it is mixed with αCN.

The aggregation of β-Lg is obvious from the scattering data at low q-values. β-Lg can self-associate or aggregate together with micellar CNs (Li, Pan, et al., 2022). While the aggregate size varies dependent on the type of CNs, the higher A_scale and lower B_scale of κCN+ β-Lg indicates that the unfolding of β-Lg and its association with micelles in the mixure with κCN is more than those in the mixture with αCN and βCN.

3.3.5. *Isothermal titration calorimetry (ITC)*

Due to the high temperature, CNs and β-Lg are in polydisperse multimeric states, making it hard to model the ITC data (Fig. 6 b-d and Fig. S14). From our DLS experiments, we already know that at 85 °C, regardless of the presence of Ca^{2+}, the majority of β-Lg in the syringe will be in a polydisperse aggregated state. In the absence of Ca^{2+} at 85 °C, αCN, βCN, and κCN are polydisperse of approximate sizes of 7, 10, and 20 nm, respectively, while in the presence of 1 mM Ca^{2+} the sizes increase to 50, 100, and 40 nm, respectively (Fig. 6a). This means that the nature of the interaction in the absence of Ca^{2+} is different from that in the presence of Ca^{2+} (depicted in Fig. 6a). Accordingly, only the thermograms and their integrated peaks were used to describe the change in CNs- β-Lg binding upon the presence of Ca^{2+} in a qualitative way.

The ITC data suggested conventional binding-saturation behavior with large initial reaction enthalpies of 15–25 kJ/mol that tapered off towards zero at molar ratios of 2–4. In all cases, the heat response from titrating β-Lg into the CNs changes from both endo- and exothermic (without Ca^{2+}) to only exothermic (with Ca^{2+}). Thus, adding Ca^{2+} renders the binding interaction enthalpically favourable.

The presence of Ca^{2+} modulates the stoichiometry and strength of the interactions inferred from the enthalpograms. For all CNs and at all β-Lg to CNs molar ratios, Ca^{2+} leads to a larger favourable (i.e. negative) interaction enthalpy, which can be due to either a change in the energetic character of the interaction or a change in stoichiometry, or both, in the presence of Ca^{2+}. The increase in the enthalpy of the interactions between β-Lg and αCN due to the presence of Ca^{2+} is more pronounced than for β-Lg and βCN and κCN, which can be due to the higher sensitivity of αCN to the presence of Ca^{2+}. From the enthalpy data, we can also conclude a higher enthalpy change due to the interaction of β-Lg with κCN than with αCN and βCN.

4. Conclusion

While the effect of heating and Ca^{2+} on the chaperone activity of CNs for β-Lg has been studied before, there are many open questions yet to be addressed. Here, we used a combination of different experimental approaches to show that the CNs and β-Lg behave differently at different temperatures and Ca^{2+} concentrations. While heat treatment affected denaturation and aggregation of β-Lg with little dependency on Ca^{2+}, αCN and βCN were influenced considerably by Ca^{2+}. By comparing the present results with previous studies, we conclude that CNs display chaperone activity through slight suppression of β-Lg unfolding and that this process is also dependent on the type of CNs. Furthermore, the chaperone activity of CNs significantly limits the aggregate formation of unfolded β-Lg in the absence of Ca^{2+}, or decreases the aggregate size in the presence of Ca^{2+}, through hydrophobic interactions (Fig. 7). Our findings thus elucidate the molecular understanding of complexation of CNs and β-Lg and contribute to the wider discussions concerning the assembly of milk proteins to provide milk-based products with different functionalities.

CRediT authorship contribution statement

Hossein Mohammad-Beigi and **Wahyu Wijaya**: Conceptualization, Investigation, Writing Original draft, Writing - Review & Editing, Visualization. **Mikkel Madsen, Yuya Hayashi, and Ruifen Li**: Investigation, Writing - Review & Editing. **Tanja Christine Jæger**, **Tijs Albert Maria Rovers, Alexander K. Buell, Jacob J.K. Kirkensgaard, and Peter Westh**: Conceptualization, Writing-review & Editing. **Anni Bygvrå Hougaard:** Project administration, Writing – review & Editing. **Richard Ipsen:** Conceptualization, Writing-review & Editing, Funding acquisition. **Birte Svensson**: Conceptualization, Supervision, Validation, Writing – review & editing, Funding acquisition. All authors discussed the results, commented on the paper, and gave approval to the manuscript's final version.

Declaration of competing interest

None. Note that Tijs Albert Maria Rovers is an employee of Arla Foods A.m.b.a. and Tanja Christine Jæger is an employee of Arla Food Ingredients Group P/S.

Data availability

Data will be made available on request.

Acknowledgment

This study is part of the Bespoke project funded by the Danish Dairy Research Foundation, Arla Foods A.m.b.a., and Chinese Scholarship Council (to R.L.). Arla Food Ingredients is acknowledged for providing useful inputs. The Carlsberg Foundation is acknowledged for funding of the ITC instrument. H.M-B., and W.W. were supported by the Bespoke project (grant 101090), M.M. by a 1/3 DTU PhD scholarship, and Y.H. by the Novo Nordisk Foundation (NNF21OC0067359). Jens Preben Morth (DTU Bioengineering) is thanked for access to the circular dichroism (CD). A.K.B. would like to acknowledge the Novo Nordisk Foundation for funding (Grant number: NNFSA170028392). SAXS data was generated via a research infrastructure at University of Copenhagen, partly funded by FOODHAY (Food and Health Open Innovation Laboratory, Danish Roadmap for Research Infrastructure). This work benefited from using the SasView application, originally developed under NSF award DMR-0520547. SasView contains code developed with funding from the European Union's Horizon 2020 research and innovation program under the SINE2020 project, grant agreement No 654000.

Appendix A. Supplementary data

Supplementary data to this article can be found online at https://doi.org/10.1016/j.foodhyd.2022.108373.

References

Anema, S. G. (2021). Heat-induced changes in caseins and casein micelles, including interactions with denatured whey proteins. *International Dairy Journal, 122*, Article 105136. https://doi.org/10.1016/j.idairyj.2021.105136

Atkins, P., & De Paula, J. (2013). *Elements of physical chemistry* (6th ed.). USA: Oxford University Press. https://doi.org/10.1002/bbpc.19920961162

Clark, A., Saunderson, D., & Suggett, A. (1981). Infrared and laser-Raman spectroscopic studies of thermally-induced globular protein gels. *International Journal of Peptide and Protein Research, 17*, 353–364. https://doi.org/10.1111/j.1399-3011.1981.tb02002.x

Dalgleish, D. G., & Corredig, M. (2012). The structure of the casein micelle of milk and its changes during processing. *Annual Review of Food Science and Technology, 3*, 449–467. https://doi.org/10.1146/annurev-food-022811-101214

Dauphas, S., Mouhous-Riou, N., Metro, B., Mackie, A., Wilde, P. J., Anton, M., et al. (2005). The supramolecular organisation of β-casein: Effect on interfacial properties. *Food Hydrocolloids, 19*, 387–393. https://doi.org/10.1016/j.foodhyd.2004.10.005

De, M., & Rotello, V. M. (2008). Synthetic "chaperones": Nanoparticle-mediated refolding of thermally denatured proteins. *Chemical Communications*, 3504–3506. https://doi.org/10.1039/b805242e

Durand, D., Gimel, J. C., & Nicolai, T. (2002). Aggregation, gelation and phase separation of heat denatured globular proteins. *Physica A: Statistical Mechanics and Its Applications, 304*, 253–265. https://doi.org/10.1016/s0378-4371(01)00514-3

Duy, C., & Fitter, J. (2006). How aggregation and conformational scrambling of unfolded states govern fluorescence emission spectra. *Biophysical Journal, 90*, 3704–3711. https://doi.org/10.1529/biophysj.105.078980

Erabit, N., Flick, D., & Alvarez, G. (2013). Effect of calcium chloride and moderate shear on β -lactoglobulin aggregation in processing-like conditions. *Journal of Food Engineering, 115*, 63–72. https://doi.org/10.1016/j.jfoodeng.2012.09.020

Etzel, M. R. (2004). Manufacture and use of dairy protein fractions. *Journal of Nutrition, 134*, 996S–1002S. https://doi.org/10.1093/jn/134.4.996s

Faizullin, D., Konnova, T., Haertlé, T., & Zuev, Y. F. (2013). Self-assembly and secondary structure of beta-casein. *Russian Journal of Bioorganic Chemistry, 39*, 366–372. https://doi.org/10.1134/s1068162013040067

Farrell, H., Qi, P., Wickham, E., & Unruh, J. (2002). Secondary structural studies of bovine caseins: Structure and temperature dependence of β-casein phosphopeptide (1-25) as analyzed by circular dichroism, FTIR spectroscopy, and analytical ultracentrifugation. *Journal of Protein Chemistry, 21*, 307–321. https://doi.org/10.1016/s0268-005x(01)00080-7

Feigin, L., Svergun, D. I., & others. (1987). *Structure analysis by small-angle X-ray and neutron scattering* (Vol. 1). Springer. https://doi.org/10.1021/jp051470o.s001

Fox, P. F. (2008). Milk: An overview. In *Milk proteins* (pp. 1–54). Elsevier. https://doi.org/10.1016/b978-0-12-374039-7.00001-5.

Fox, P. F., & McSweeney, P. L. (2013). *Advanced dairy chemistry: Volume 1: Proteins*. parts A\&B. Springer. https://doi.org/10.1007/978-1-4614-4714-6

Guyomarc'h, F., Nono, M., Nicolai, T., & Durand, D. (2009). Heat-induced aggregation of whey proteins in the presence of κ-casein or sodium caseinate. *Food Hydrocolloids, 23*, 1103–1110. https://doi.org/10.1016/j.foodhyd.2008.07.001

Haque, Z., & Kinsella, J. E. (1988). Interaction between heated κ-casein and β-lactoglobulin: Predominance of hydrophobic interactions in the initial stages of complex formation. *Journal of Dairy Research, 55*, 67–80. https://doi.org/10.1017/s0022029900025863

Holt, C., Carver, J., Ecroyd, H., & Thorn, D. (2013). Invited review: Caseins and the casein micelle: Their biological functions, structures, and behavior in foods. *Journal of Dairy Science, 96*, 6127–6146. https://doi.org/10.3168/jds.2013-6831

Iametti, S., De Gregori, B., Vecchio, G., & Bonomi, F. (1996). Modifications occur at different structural levels during the heat denaturation of β-lactoglobulin. *European Journal of Biochemistry, 237*(1), 106–112. https://doi.org/10.1111/j.1432-1033.1996.0106n.x

Kehoe, J., & Foegeding, E. (2011). Interaction between β-casein and whey proteins as a function of pH and salt concentration. *Journal of Agricultural and Food Chemistry, 59*, 349–355. https://doi.org/10.1021/jf103371g

Kehoe, J., & Foegeding, E. (2014). The characteristics of heat-induced aggregates formed by mixtures of β-lactoglobulin and β -casein. *Food Hydrocolloids, 39*, 264–271. https://doi.org/10.1016/j.foodhyd.2014.01.019

Kenkare, D., Morr, C., & Gould, I. (1964). Factors affecting the heat aggregation of proteins in selected skimmilk sera. *Journal of Dairy Science, 47*, 947–953. https://doi.org/10.3168/jds.s0022-0302(64)88817-2

Kristiansen, K., Otte, J., Ipsen, R., & Qvist, K. (1998). Large-scale preparation of β-lactoglobulin A and B by ultrafiltration and ion-exchange chromatography. *International Dairy Journal, 8*, 113–118. https://doi.org/10.1016/s0958-6946(98)00028-4

Lê, S., Josse, J., & Husson, F. (2008). FactoMineR: an R package for multivariate analysis. *Journal of Statistical Software, 25*, 1–18. https://doi.org/10.18637/jss.v025.i01

Li, M., Auty, M. A., Crowley, S. V., Kelly, A. L., O'Mahony, J. A., & Brodkorb, A. (2019). Self-association of bovine β-casein as influenced by calcium chloride, buffer type and temperature. *Food Hydrocolloids, 88*, 190–198. https://doi.org/10.1016/j.foodhyd.2018.09.035

Li, R., Jæger, T. C., Rovers, T. A. M., Svensson, B., Ipsen, R., Kirkensgaard, J. J., et al. (2022). In situ SAXS study of non-fat milk model systems during heat treatment and acidification. *Food Research International, 157*, Article 111292. https://doi.org/10.1016/j.foodres.2022.111292

Li, H., Pan, Y., Yang, Z., Rao, J., & Chen, B. (2022). Modification of β-lactoglobulin by phenolic conjugations: Protein structural changes and physicochemical stabilities of stripped hemp oil-in-water emulsions stabilized by the conjugates. *Food Hydrocolloids, 128*, Article 107578. https://doi.org/10.1016/j.foodhyd.2022.107578

Liyanaarachchi, W., & Vasiljevic, T. (2018). Caseins and their interactions that modify heat aggregation of whey proteins in commercial dairy mixtures. *International Dairy Journal, 83*, 43–51. https://doi.org/10.1016/j.idairyj.2018.03.006

Marchesseau, S., Mani, J., Martineau, P., Roquet, F., Cuq, J., & Pugniere, M. (2002). Casein interactions studied by the surface plasmon resonance technique. *Journal of Dairy Science, 85*, 2711–2721. https://doi.org/10.3168/jds.s0022-0302(02)74358-0

Matsudomi, N., Kanda, Y., Yoshika, Y., & Moriwaki, H. (2004). Ability of α-casein to suppress the heat aggregation of ovotransferrin. *Journal of Agricultural and Food Chemistry, 52*, 4882–4886. https://doi.org/10.1021/jf030802o

McKenzie, G., Norton, R., & Sawyer, W. (1971). Heat-induced interaction of β-lactoglobulin and κ-casein. *Journal of Dairy Research, 38*, 343–351. https://doi.org/10.3168/jds.s0022-0302(63)89276-0

McSweeney, P. L., & Fox, P. F. (2013). *Advanced dairy chemistry: Volume 1A: Proteins: Basic aspects*. Springer Science \& Business Media. https://doi.org/10.1007/978-1-4614-4714-6

Mekhloufi, G., Vilamosa, N., & Agnely, F. (2022). Nanoemulsion stabilized by β-lactoglobulin: A promising strategy to encapsulate curcumin for topical delivery. *Materials Today Proceedings*. https://doi.org/10.1016/j.matpr.2021.12.489

Mercadante, D., Melton, L. D., Norris, G. E., Loo, T. S., Williams, M. A., Dobson, R. C., et al. (2012). Bovine β-lactoglobulin is dimeric under imitative physiological conditions: Dissociation equilibrium and rate constants over the pH range of 2.5-7.5. *Biophysical Journal, 103*(2), 303–312. https://doi.org/10.1016/j.bpj.2012.05.041

Minic, S., Annighöfer, B., Hélary, A., Hamdane, D., Hoa, G. H. B., Loupiac, C., et al. (2020). Effect of ligands on HP-induced unfolding and oligomerization of β-lactoglobulin. *Biophysical Journal, 119*(11), 2262–2274. https://doi.org/10.1101/2020.06.29.177972

Morgan, P. E., Treweek, T. M., Lindner, R. A., Price, W. E., & Carver, J. A. (2005). Casein proteins as molecular chaperones. *Journal of Agricultural and Food Chemistry, 53*, 2670–2683. https://doi.org/10.1201/9781482283440-21

Peixoto, P. D., Trivelli, X., André, C., Moreau, A., & Delaplace, G. (2018). Formation of β-lactoglobulin aggregates from quite, unfolded conformations upon heat activation. *Langmuir, 35*, 446–452. https://doi.org/10.1021/acs.langmuir.8b03459.s001

Petit, J., Herbig, A.-L., Moreau, A., & Delaplace, G. (2011). Influence of calcium on β-lactoglobulin denaturation kinetics: Implications in unfolding and aggregation mechanisms. *Journal of Dairy Science, 94*(12), 5794–5810. https://doi.org/10.3168/jds.2011-4470

Portnaya, I., Khalfin, R., & Danino, D. (2021). Interplay of interactions between micelles and fibrils of casein proteins. *Food Hydrocolloids, 120*, Article 106950. https://doi.org/10.1016/j.foodhyd.2021.106950

Rodrigues, R. M., Claro, B., Bastos, M., Pereira, R. N., Vicente, A. A., & Petersen, S. B. (2020). Multi-step thermally induced transitions of β-lactoglobulin-An in situ spectroscopy approach. *International Dairy Journal, 100*, Article 104562. https://doi.org/10.1016/j.idairyj.2019.104562

Sava, N., Van der Plancken, I., Claeys, W., & Hendrickx, M. (2005). The kinetics of heat-induced structural changes of beta-lactoglobulin. *Journal of Dairy Science, 88*, 1646–1653. https://doi.org/10.3168/jds.s0022-0302(05)72836-8

Steinhauer, T., Kulozik, U., & Gebhardt, R. (2014). Structure of milk protein deposits formed by casein micelles and β-lactoglobulin during frontal microfiltration. *Journal of Membrane Science, 468*, 126–132. https://doi.org/10.1016/j.memsci.2014.05.027

Thorn, D. C., Meehan, S., Sunde, M., Rekas, A., Gras, S. L., MacPhee, C. E., et al. (2005). Amyloid fibril formation by bovine milk κ-casein and its inhibition by the molecular chaperones α-and β-casein. *Biochemistry, 44*, 17027–17036. https://doi.org/10.1021/bi051352r

Uhrinová, S., Smith, M. H., Jameson, G. B., Uhrin, D., Sawyer, L., & Barlow, P. N. (2000). Structural changes accompanying pH-induced dissociation of the β-lactoglobulin dimer. *Biochemistry, 39*(13), 3565–3574. https://doi.org/10.2210/pdb1dv9/pdb

Wijaya, W., Khan, S., Madsen, M., Møller, M. S., Rovers, T. A. M., Jæger, T. C., et al. (2020). Tunable mixed micellization of β-casein in the presence of κ-casein. *Food Hydrocolloids*. , Article 106459. https://doi.org/10.1016/j.foodhyd.2020.106459

Yang, S., Tyler, A. I., Ahrné, L., & Kirkensgaard, J. J. K. (2021). Skimmed milk structural dynamics during high hydrostatic pressure processing from in situ SAXS. *Food Research International, 147*, Article 110527. https://doi.org/10.1016/j.foodres.2021.110527

Yousefi, R., Shchutskaya, Y. Y., Zimny, J., Gaudin, J.-C., Moosavi-Movahedi, A. A., Muronetz, V. I., et al. (2009). Chaperone-like activities of different molecular forms of β-casein. Importance of polarity of N-terminal hydrophilic domain. *Biopolymers: Original Research on Biomolecules, 91*, 623–632. https://doi.org/10.1002/bip.21190

Zhang, S., Li, X., Zheng, L., Zheng, X., Yang, Y., Xiao, D., et al. (2022). Encapsulation of phenolics in β-lactoglobulin: Stability, antioxidant activity, and inhibition of advanced glycation end products. *LWT, 113437*. https://doi.org/10.1016/j.lwt.2022.113437